

Supplementary Information

High-Resolution Magnetization Transfer Imaging of *Post-Mortem* Marmoset Brain: Comparisons with Relaxometry and Histology

Henrik Marschner¹, André Pampel¹, Roland Müller¹, Katja Reimann², Nicolas Bock³,
Markus Morawski², Stefan Geyer¹, Harald E. Möller^{1,*}

¹ *Max Planck Institute for Human Cognitive and Brain Sciences, Stephanstraße 1a, 04103 Leipzig, Germany*

² *Paul Flechsig Institute of Brain Research, Liebigstraße 19, 04103 Leipzig, Germany*

³ *McMaster University, Department of Psychology, Neuroscience & Behaviour, 1280 Main Street West, Hamilton, ON L8S4K1, Canada*

Abbreviations

2D = two-dimensional; 3D = three-dimensional; 3V = 3rd ventricle; A24 = area 24; ac = anterior commissure; Am = amygdaloid nuclei; BSB = binary spin bath; c = central part; cc = corpus callosum; Cd = caudate nucleus; Cl = claustrum; cr = corona radiata; ec = external capsule; EN = endopiriform nuclei; ex = extreme capsule; FLASH = fast low-angle shot; FOV = field of view; GM = gray matter; ic = internal capsule; Ins = insula; IOD = integrated optical density; l = lateral part; lf = lateral fissure; LV = lateral ventricle; M1 = primary motor cortex; MBP = myelin basic protein; ME = multi echo; MP2RAGE = magnetization-prepared 2 rapid gradient echoes; MR = magnetic resonance; MRI = magnetic resonance imaging; MT = magnetization transfer; och = optic chiasm; PaC = parietal cortex; PBS = phosphate-buffered saline; PCB = printed circuit board; Pu = putamen; qMTI = quantitative magnetization transfer imaging; RF = radiofrequency; ROI = region of interest; S1 = primary somatosensory cortex; SNR = signal-to-noise ratio; V1 = primary visual cortex; VP = ventral pallidum; WM = white matter.

Mathematical Symbols

A :	absorbance;
a :	normalized absorbance;
a, b :	superscripts denoting the free and the semisolid pool, respectively;
app:	subscript denoting an apparent quantity;
\mathbf{B}_0 :	static magnetic field vector;
B_0 :	static magnetic field amplitude;
B_1^+ :	RF transmit magnetic field amplitude;
$B_{1,\max}^+$:	RF transmit magnetic field peak amplitude;
$B_{1,\text{rms}}^+$:	root-mean-squared RF transmit magnetic field amplitude;
C :	capacitance;
C_m :	matching capacitance;
C_t :	tuning capacitance;
C^\pm :	coefficients;
c_1, c_0, c'_0 :	linear coefficients in multivariate regression analysis;
E_1 :	exponential longitudinal relaxation factor;
F :	ratio of mean squared error and mean squared residuals;
\mathcal{F} :	pool-size ratio M_0^b / M_0^a ;
$_{\text{Fe}}$:	subscript denoting Perls' stain for ferric iron (Fe^{3+});
f :	fraction of the total tissue mass;
f_{\max}^m :	maximum myelin fraction of the total tissue mass;
g^b :	absorption lineshape function of the semisolid pool;
I :	transmitted intensity;
I_0 :	incident intensity;
i :	position index;
$^{iew}, ^{mw}$:	superscripts denoting intra-/extracellular and myelin water, respectively;
M_0 :	equilibrium magnetization;
M_z :	longitudinal magnetization;
$_{\text{MBP}}$:	subscript denoting MBP immunostaining;
MTR	magnetization transfer ratio;
MWF	myelin water fraction;
m, nm :	superscripts denoting myelin and non-myelin dry matter, respectively;
$_{\text{my}}$:	subscript denoting Gallyas' silver stain for myelin;
N_{av} :	number of averages;
n :	number of voxels;
p :	error probability;
Q :	quality factor;
R :	exchange rate constant;
R_1 :	longitudinal relaxation rate;
R_1^{obs} :	observed longitudinal relaxation rate;
R_1^W :	longitudinal relaxation rate of water;
R_2 :	transverse relaxation rate;
R_2^* :	effective transverse relaxation rate;
R_{RF} :	RF saturation rate;
RSME:	root mean-squared error;
r :	Pearson correlation coefficient;
r_{adj}^2 :	adjusted coefficient of determination;

r_c :	cosine fraction of the Tukey window;
S :	signal voltage;
S_0 :	signal voltage generated by a 90° pulse to the fully relaxed magnetization;
SD:	standard deviation;
T_1 :	longitudinal relaxation time;
T_1^{obs} :	observed longitudinal relaxation time;
T_2 :	transverse relaxation time;
T_2^* :	effective transverse relaxation time;
TE:	echo time;
ΔTE :	inter-echo time;
TI:	inversion time;
TR:	repetition time;
x, y, z :	Cartesian coordinates;
$y(x_1, x_2, \dots)$:	function of the variables x_1, x_2, \dots ;
y_0 :	constant term;
α :	imaging pulse flip angle;
ϑ :	polar angle (in the magnet coordinate system);
ϵ_1, ϵ_0 :	linear coefficients describing the correlation of a_{my} and a_{Fe} ;
η :	power-law coefficient;
κ :	power-law exponent;
λ_{\pm} :	apparent relaxation rates;
σ :	scaling factor;
τ_p :	pulse duration;
φ :	azimuth angle (in the magnet coordinate system);
Ω :	off-resonance angular frequency;
ω_1 :	RF pulse amplitude (in rad/s);
$\omega_{1,\text{max}}$:	RF pulse peak amplitude (in rad/s);
\bar{x} :	mean value of the quantity x .

Supplementary Table S1. Pearson correlation coefficients, r , for pairwise comparisons of histology results (normalized IOD of Gallyas' myelin stain, MBP immunostain, and Perls' iron stain), MT parameters (pool-size ratio $\mathcal{F} = M_0^b/M_0^a$ and exchange rate), and relaxation rates R_1^{obs} (at 3 T and 7 T) and R_2^* . The upper-right (gray background) and lower-left (white background) parts of the correlation diagram show results from separate analyses in all GM ($n = 4,964$) and all WM voxels ($n = 1,538$; including optic chiasm), respectively, which were performed without outlier removal. Significant correlations (after Bonferroni correction) are indicated in bold, numbers in brackets indicate insignificant correlations.

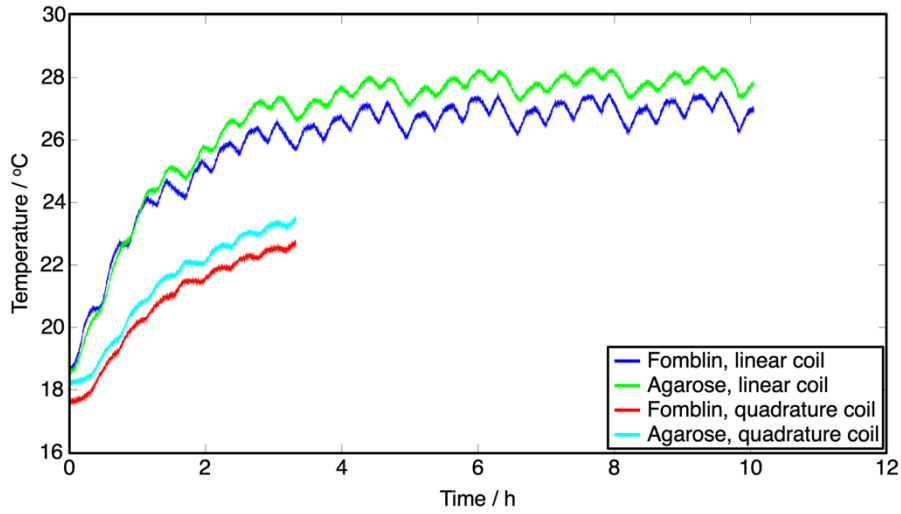
r	a_{my}	a_{MBP}	a_{Fe}	\mathcal{F}	RM_0^a	$R_{1,3T}^{\text{obs}}$	$R_{1,7T}^{\text{obs}}$	R_2^*	
a_{my}		0.894***	0.568***	0.543***	0.159***	0.633***	0.675***	0.474***	GM
a_{MBP}	(0.041)		0.626***	0.569***	0.242***	0.672***	0.711***	0.573***	
a_{Fe}	0.411***	(0.056)		0.452***	0.282***	0.614***	0.630***	0.669***	
\mathcal{F}	0.555***	(-0.060)	0.463***		-0.329***	0.653***	0.683***	0.458***	
RM_0^a	0.094***	0.112***	0.311***	-0.142***		0.232***	0.181***	0.285***	
$R_{1,3T}^{\text{obs}}$	0.571***	(0.076)	0.647***	0.719***	0.320***		0.871***	0.655***	
$R_{1,7T}^{\text{obs}}$	0.619***	(0.022)	0.645***	0.752***	0.200***	0.872***		0.739***	
R_2^*	0.522***	(-0.027)	0.637***	0.629***	0.235***	0.748***	0.824***		
	WM								

Supplementary Table S2. Coefficients (\pm SD) obtained by fitting the variation of estimated BSB model parameters upon changing the assumed fixed value for R_1^b in the range from 1 s⁻¹ and 8 s⁻¹ to a power law, $y(R_1^b) = y_0 + \eta(R_1^b)^\kappa$. Data for four arbitrarily selected voxels in the primary somatosensory cortex (S1), amygdaloid nuclei (Am), anterior commissure (ac) and internal capsule (ic) are included as well as the region-averaged exponent, $\langle \kappa \rangle$.

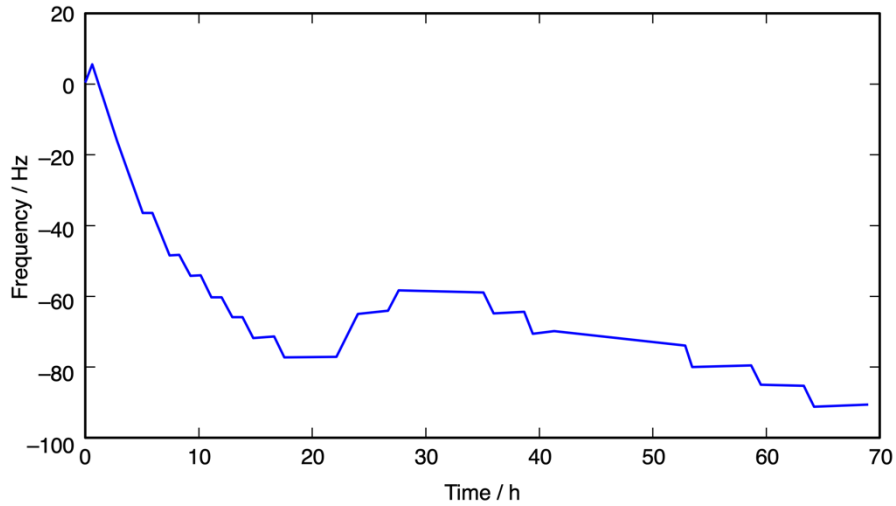
y	Region	y_0	η	κ	$\langle \kappa \rangle$
\mathcal{F}	S1	0.10596±0.00017	0.001116±0.000043	1.837±0.018	1.93 ±0.13
	Am	0.07560±0.00013	0.000924±0.000034	1.806±0.017	
	ac	0.17872±0.00031	0.001117±0.000059	2.083±0.025	
	ic	0.21618±0.00031	0.001370±0.000066	1.992±0.023	
RM_0^a/s	S1	46.973±0.063	-5.167±0.045	0.8395±0.0033	0.833±0.016
	Am	42.162±0.068	-4.949±0.050	0.8121±0.0038	
	ac	51.814±0.092	-6.453±0.067	0.8312±0.0040	
	ic	59.512±0.094	-6.917±0.067	0.8486±0.0038	
R_1^a/s	S1	3.12736±0.00036	-0.08805±0.00021	1.0973 ±0.0010	1.089±0.012
	Am	2.29821±0.00017	-0.06132±0.00010	1.08312±0.00070	
	ac	3.77771±0.00030	-0.16074±0.00018	1.07568±0.00046	
	ic	4.76717±0.00063	-0.18954±0.00037	1.10060±0.00081	
T_2^a/ms	S1	26.3546±0.0043	0.04802±0.00092	1.9792±0.0091	2.16 ±0.30
	Am	34.0947±0.0056	0.0803 ±0.0014	1.8589±0.0082	
	ac	19.5562±0.0047	0.03004±0.00068	2.268 ±0.011	
	ic	15.9747±0.0019	0.01124±0.00018	2.5375±0.0079	
$T_2^b/\mu s$	S1	9.71993±0.00017	0.005066±0.000071	1.4352±0.0063	1.50 ±0.19
	Am	8.34549±0.00013	0.008119±0.000064	1.2610±0.0034	
	ac	9.47898±0.00022	0.004348±0.000079	1.5745±0.0083	
	ic	9.73699±0.00021	0.002503±0.000064	1.717 ±0.012	

Supplementary Table S3. F -statistic results including the root mean-squared error (RMSE), adjusted coefficient of determination (r_{adj}^2) and F -value ($p < 0.001$) for comparisons of bivariate linear regression models $y(x_\alpha, x_\beta) = c_1^\alpha x_\alpha + c_1^\beta x_\beta + c_0$ (see Table 4) to corresponding linear models $y(x_{\alpha,\beta}) = c_1^{\alpha,\beta} x_{\alpha,\beta} + c_0^{\alpha,\beta}$ (n.s. = not significant).

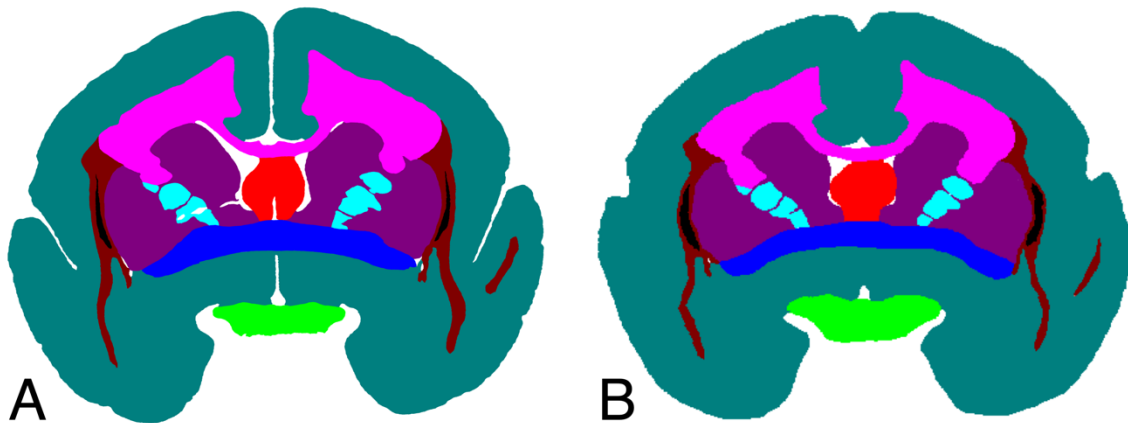
y	x_α	x_β	Whole slice				GM mask				WM mask			
			RMSE	r_{adj}^2	F_α	F_β	RMSE	r_{adj}^2	F_α	F_β	RMSE	r_{adj}^2	F_α	F_β
$R_{1,3T}^{\text{obs}}/\text{s}^{-1}$	a_{my}	a_{Fe}	0.178	0.714	2,580	1,667	0.146	0.496	940	1,171	0.247	0.571	627	230
$R_{1,3T}^{\text{obs}}/\text{s}^{-1}$	\mathcal{F}	a_{Fe}	0.155	0.780	2,345	3,968	0.137	0.554	1,420	1,973	0.224	0.645	580	469
$R_{1,7T}^{\text{obs}}/\text{s}^{-1}$	a_{my}	a_{Fe}	0.164	0.759	2,661	2,649	0.140	0.546	979	1,625	0.201	0.576	602	265
$R_{1,7T}^{\text{obs}}/\text{s}^{-1}$	\mathcal{F}	a_{Fe}	0.143	0.816	2,651	5,295	0.132	0.596	1,598	2,444	0.185	0.642	551	483
R_2^*/s^{-1}	a_{my}	a_{Fe}	5.73	0.688	3,472	688	4.76	0.461	2,175	119	7.52	0.442	380	133
R_2^*/s^{-1}	\mathcal{F}	a_{Fe}	5.3	0.737	3,035	1,925	4.6	0.490	2,476	408	7.3	0.472	329	192
\mathcal{F}	a_{my}	a_{Fe}	0.025	0.606	953	1,694	0.017	0.325	223	890	0.035	0.227	80	106
RM_0^a/s^{-1}	a_{my}	a_{Fe}	3.13	0.104	451	20	2.94	0.079	294	<i>n.s.</i>	3.92	0.171	174	<i>n.s.</i>



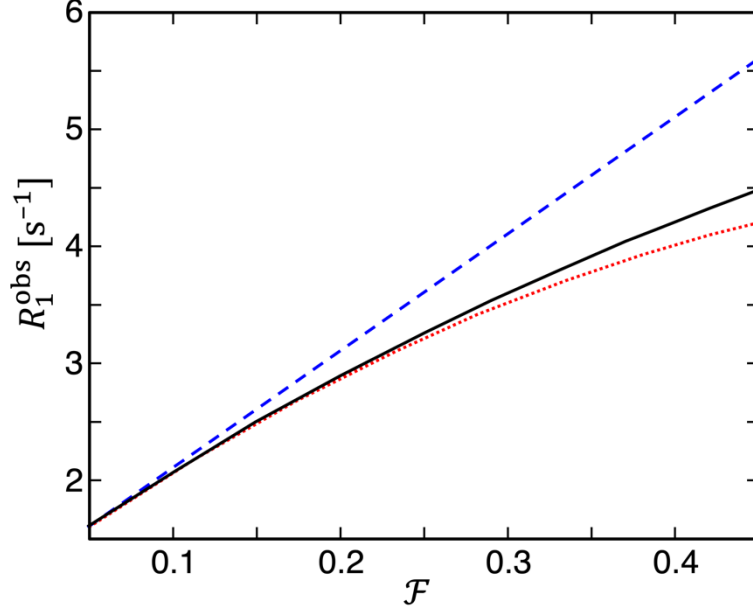
Supplementary Figure S1. Change of the sample temperature with in experiments performed in spherical phantoms filled with Fomblin (blue and red lines) or agarose (green and turquoise lines). The temperature was constantly monitored during acquisitions with the qMRI protocol using a fiberoptic sensor inserted inside the sample. A reasonably stable temperature was obtained after approximately 3 hours of scanning with residual fluctuations depending on the actual RF power of the MT pulse. A substantial reduction in heating due to the deposited RF energy was achieved with the quadrature Helmholtz coil (red and turquoise lines) as compared to a simple linear Helmholtz coil (blue and green lines).



Supplementary Figure S2. Variation of the resonance frequency during approximately 70 hours of continuous scanning with the qMTI protocol. The field drift is most pronounced during the initial 10 hours and probably due to heating of the gradient coil.



Supplementary Figure S3. Manually generated masks with different tissue classes on (A) magnified silver stain (see Figure 3A) and (B) high-resolution 7-T FLASH images.



Supplementary Figure S4. Simulated variation of $R_1^{\text{obs}}(\mathcal{F}, a_{\text{Fe}})$ based on the BSB model, Eq. A8, plotted as a function of \mathcal{F} , as well as first (linear; blue broken line) and second (quadratic; red dotted line) Taylor expansion (see below). The following parameters were used for these calculations: $R_1^b = 5 \text{ s}^{-1}$, $R_1^w = 1.6 \text{ s}^{-1}$, $RM_0^a = 25 \text{ s}^{-1}$, and $c_1^{\text{Fe}} = 1.4 \text{ s}^{-1}$. a_{Fe} was assumed to vary linearly with \mathcal{F} as $a_{\text{Fe}} = 5\mathcal{F} - 0.35$, which is similar to the results in Table 3.

BSB model-based estimation of R_1^{obs} ; exact result (see Appendix B):

$$R_1^{\text{obs}}(\mathcal{F}, a_{\text{Fe}}) = \frac{1}{2} \left\{ R_1^b + R_1^w + c_1^{\text{Fe}} a_{\text{Fe}} + RM_0^a (1 + \mathcal{F}) - \sqrt{[R_1^b - R_1^w - c_1^{\text{Fe}} a_{\text{Fe}} + RM_0^a (1 - \mathcal{F})]^2 + 4(RM_0^a)^2 \mathcal{F}} \right\}. \quad (\text{S1})$$

First-order Taylor expansion:

$$R_1^{\text{obs}}(\mathcal{F}, a_{\text{Fe}}) \approx R_1^w + \frac{(R_1^b - R_1^w) RM_0^a}{R_1^b - R_1^w + RM_0^a} \cdot \mathcal{F} + c_1^{\text{Fe}} a_{\text{Fe}}. \quad (\text{S2})$$

Second-order Taylor expansion:

$$R_1^{\text{obs}}(\mathcal{F}, a_{\text{Fe}}) \approx R_1^w + \frac{(R_1^b - R_1^w) RM_0^a}{R_1^b - R_1^w + RM_0^a} \cdot \mathcal{F} + c_1^{\text{Fe}} a_{\text{Fe}} - \frac{(R_1^b - R_1^w)(RM_0^a)^3}{(R_1^b - R_1^w + RM_0^a)^3} \cdot \mathcal{F}^2 - \frac{(RM_0^a)^2}{(R_1^b - R_1^w + RM_0^a)^2} \cdot \mathcal{F} \cdot c_1^{\text{Fe}} a_{\text{Fe}}. \quad (\text{S3})$$